Regulatory role of β-arrestin-2 in cholesterol processing in cystic fibrosis epithelial cells

Mary E. Manson,[1,*] Deborah A. Corey,[1,†] Ilya Bederman,[†] James D. Burgess,[*] and Thomas J. Kelley[2,*,†]

Departments of Chemistry* and Pediatrics,† Case Western Reserve University, Cleveland, OH

Abstract Cystic fibrosis (CF) cells exhibit an increase in the protein expression of β-arrestin-2 (βarr2) coincident with perinuclear accumulation of free cholesterol. Arrestins are proteins that both serve as broad signaling regulators and contribute to G-protein coupled receptor internalization after agonist stimulation. The hypothesis of this study is that βarr2 is an important component in the mechanisms leading to cholesterol accumulation characteristic of CF cells. To test this hypothesis, epithelial cells stably expressing GFP-tagged βarr2 (βarr2-GFP) and respective GFP-expressing control cells (cont-GFP) were analyzed by filipin staining. The βarr2-GFP cells show a late endosomal/lysosomal cholesterol accumulation that is identical to that seen in CF cells. This βarr2-mediated accumulation is sensitive to *Rp*-cAMPS treatment, and depleting βarr2 expression in CF-model cells by shRNA alleviates cholesterol accumulation compared with controls. *Cftr/βarr2* double knockout mice also exhibit wild-type (WT) levels of cholesterol synthesis, and WT profiles of signaling protein expression have previously been shown to be altered in CF due to cholesterol-related pathways. These data indicate a significant regulatory role for βarr2 in the development of CF-like cholesterol accumulation and give further insight into cholesterol processing mechanisms. An impact of βarr2 expression on Niemann-Pick type C-1 (NPC1)-containing organelle movement is proposed as the mechanism of βarr2-mediated alterations on cholesterol processing. It is concluded that βarr2 expression contributes to altered cholesterol trafficking observed in CF cells.—Manson, M. E., D. A. Corey, I. Bederman, J. D. Burgess, and T. J. Kelley. **Regulatory role of β-arrestin-2 in cholesterol processing in cystic fibrosis epithelial cells. *J. Lipid Res.* 2012.** 53: **1268–1276.**

Supplementary key words cAMP • cell signaling • cholesterol • cholesterol/biosynthesis • cholesterol/trafficking • endocytosis

Cystic fibrosis (CF) is caused by the loss of cystic fibrosis transmembrane conductance regulator (CFTR) function, resulting in dysregulation of ion transport, abnormal inflammatory response signaling, and altered cholesterol homeostasis both in CF-cell models and in vivo (1–11). There are three different manifestations of the CF cholesterol phenotype: perinuclear free-cholesterol accumulation, increased membrane cholesterol content, and increased de novo cholesterol synthesis (10, 11). Previously we demonstrated that accumulated perinuclear cholesterol in CF-cell models is reversible in the presence of the cAMP binding competitor *Rp*-cAMPS, and it colocalizes with internalized β2-adrenergic receptor (β2-AR) (12). These findings implicate the arrestin/G-protein coupled receptor kinase (GRK) pathway as a potential regulator of the CF cholesterol phenotype. The same study demonstrated increased expression of β-arrestin-2 (βarr2) in CF-cell models, *Cftr* $^{-/-}$ mouse nasal epithelia (MNE), and nasal scrapes obtained from CF patients compared with respective controls (12). The hypothesis to test in this study is that expression of βarr2 in CF cells mediates the development of *Rp*-cAMPS-sensitive cholesterol accumulation.

Arrestins are multifunctional proteins that influence several cell regulatory pathways. The function initially identified was as regulators of G-protein coupled receptors (GPCR) in concert with GRKs. Arrestins and GRKs act as silencers of a variety of GPCRs, such as β-adrenergic receptors (β-AR), rhodopsin, and CXCRs (13). Phosphorylated by GRKs, arrestins bind to GPCRs, inhibiting interactions with G-protein subunits and stimulating receptor internalization (6). In addition to the regulation of GPCRs, arrestins have been linked to cell signaling regulation, and they affect the activity of c-Src, RhoA, PI3 kinase, MAPKs, and NF-κB (14–17). Arrestin- and GRK-mediated internalization of receptors utilizes the late endosomal/lysosomal

This work was supported by a grant from the Cystic Fibrosis Foundation and by National Institutes of Health Grants HL-080319 and EB-009481. Technical support was provided by core facilities of the Cystic Fibrosis Center (P30-DK-27651). Its contents are solely the responsibility of the authors and do not necessarily represent the official views of the National Institutes of Health.

Manuscript received 27 October 2011 and in revised form 23 March 2012.

Published, JLR Papers in Press, April 22, 2012
DOI 10.1194/jlr.M021972

Abbreviations: β2-AR, β2-adrenergic receptor; βarr2, β-arrestin-2; βarr2-GFP, GFP-tagged βarr2 cell; CF, cystic fibrosis; CFTR, cystic fibrosis transmembrane conductance regulator; DKO, double knockout; cont-GFP, GFP-expressing control cell; GPCR, G-protein coupled receptor; GRK, G-protein coupled receptor kinase; MNE, mouse nasal epithelia; NOS2, nitric oxide synthase 2; NPC1, Niemann-Pick type C-1; WT, wild-type.

[1] M. E. Manson and D. A. Corey contributed equally to this work.
[2] To whom correspondence should be addressed.
e-mail: thomas.kelley@case.edu

Copyright © 2012 by the American Society for Biochemistry and Molecular Biology, Inc.

This article is available online at http://www.jlr.org

trafficking, as does internalized cholesterol. It is postulated that the chronic increased expression of βarr2 could disrupt endosomal trafficking and lead to cholesterol accumulation. There is evidence that the arrestin/GRK pathway is upregulated in CF cells, independent of previous cholesterol studies. Barnes and colleagues have demonstrated that GRK2 and GRK5 are overexpressed in CF lung tissue and that, consistent with this finding, expression levels of the β2-AR are reduced at the cell surface in CF samples (18). These findings by Mak et al. confirm those reported by Sharma and Jeffery that also demonstrate reduced β2-AR expression at the surface of CF lung cells (19). The broader implication of this emphasis of the arrestin/GRK pathway on CF cells is unclear. The fate of other internalized GPCR proteins and how a disruption in the internalization and recycling pathway may affect cellular functions have not been examined.

In this study, the impact of βarr2 expression on *Rp*-cAMPS-sensitive cholesterol phenotype is examined. It is demonstrated here that stable expression of βarr2 in epithelial cells recapitulates the cholesterol accumulation phenotype characteristic of CF cells. Also, depletion of βarr2 expression in CF cells with shRNA eliminates the cholesterol accumulation. *Cftr/βarr2* double knockout (DKO) mice revert elevated de novo cholesterol synthesis in CF mouse models to wild-type (WT) levels, providing in vivo support of the role of βarr2 in CF-related cholesterol regulation. It is also demonstrated that endosomal trafficking is impaired in CF cells and that *Rp*-cAMPS treatment improves organelle mobility, providing a mechanistic avenue for further study. These data provide mechanistic insight into what regulates the cholesterol phenotype in CF and identify an important pathway that could have significant impact on pathological processes in CF disease.

MATERIALS AND METHODS

Cell culture

Human epithelial 9/HTEo− cells overexpressing the CFTR regulatory domain (pCEPR) and mock-transfected 9/9/HTEo− cells (pCEP) were a generous gift from the lab of Dr. Pamela B. Davis (Case Western Reserve University, Cleveland, OH). 9/9/HTEo− cells were developed originally by Dr. Dieter Gruenert (University of California, San Francisco, CA). These cells were chosen for use as they are human tracheal epithelial cells that grow well in culture (described below) and contain WT CFTR. The pCEPR model allows for studies in a model of chronic CFTR inhibition without the impact of ΔF508 CFTR misfolding. Cells were cared for as previously described (20). IB3-1 cells (ΔF508/W1282×; CF phenotype) and S9 cells (IB3-1 cells stably transfected with the full-length wild-type CFTR; control) were a generous gift from Pamela L. Zeitlin (Johns Hopkins University, Baltimore, MD). The S9/IB3 cell model was chosen because it provides a model of corrected CFTR. Used in conjunction with the pCEP/pCEPR cells, we are able to examine a WT cell with inhibited CFTR and a CF cell with corrected CFTR to examine the inherent impact of CFTR on signaling regulation. These cells were grown at 37°C in 95% O_2–5% CO_2 on Falcon 10 cm diameter tissue culture dishes (Biosource International, Camarillo, CA) in LHC-8 basal medium (Biofluids, Camarillo, CA) with 5% FBS. The βarr2-GFP cells and control-GFP cells were created in-house using a βarr2-pEGFP-N1 construct and a control-pEGFP-N1 construct, generous gifts from Dr. Robert Lefkowitz (Duke University, Durham, NC) and Dr. Mitchell Drumm (Case Western Reserve University, Cleveland, OH), respectively. Human epithelial 9/9/HTEo− cells stably transfected with βarr2-pEGFP-N1 (βarr2-GFP) and control-pEGFP-N1 (control-GFP) were grown at 37°C in 95% O_2–5% CO_2 on Falcon 10 cm diameter tissue culture dishes (Biosource International) in Dulbecco's modified Eagle's medium (DMEM; Gibco, Carlsbad, CA) with 10% FBS containing 0.04 mM HEPES, 2 mM L-glutamine, 1 U/ml penicillin/streptomycin, and 600 μg/ml G418 (selection drug). Cells treated with 50 μM *Rp*-cAMPS (BioMol, Farmingdale, NY) were exposed between 24 and 72 h. Cells treated with 100 μM 8-Br cAMP (CalBiochem, San Diego, CA) were exposed between 48 and 72 h.

Filipin staining

Cells were treated as previously described by Kruth and colleagues (21). Briefly, cells were grown to 75–90% confluency on Fisher brand glass coverslips. Cells were rinsed three times with PBS (138 mM NaCl, 15 mM Na_2HPO_4, 1.5 mM KCl, and 2.5 mM KH_2PO_4) and then fixed using 2% paraformaldehyde for ∼30 min. Cells were rinsed three more times with PBS and then incubated with 0.05 mg/ml filipin (Sigma-Aldrich, St. Louis, MO) in PBS for 1 h on a shaker in the dark. Filipin is a bacterial product that binds to free cholesterol and fluoresces in the ultraviolet range when bound. These properties allow for the visualization of cholesterol localization in fixed cells. Filipin was dissolved freshly in dimethylsulfoxide before each experiment. Cells were again rinsed three times in PBS before coverslips were mounted using Slow-Fade Light antifade (Molecular Probes, Eugene, OR) on slides. Cells were visualized in the UV range using a wide-field microscope with a 40× objective on a Zeiss Axiovert 200 and Metamorph software.

Western immunoblotting

Antibodies were obtained as follows: actin (Sigma), RhoA and βarr2 (Santa Cruz Biotechnology), and nitric oxide synthase 2 (NOS2; BD Transduction Laboratories). Protein samples were prepared in 60 mm diameter tissue culture dishes of cultured cells in ice-cold RIPA buffer (25 mM Tris, 15 mM NaCl, 1% Nonidet P-40, 0.5% sodium deoxycaolate, 0.1% sodium dodecyl sulfate) for 30 min at 4°C while shaking. Cell lysates were microcentrifuged at 4°C at 14,000 rpm for 10 min. Proteins were separated using SDS-PAGE containing 30–40 μg protein on a 7.5% acrylamide gel. The samples were transferred to an Immobilon-P membrane (Millipore, Bedford, MA) at 15 V for 30 min. The blots were blocked for 1 h at room temperature in 10% nonfat dehydrated milk in PBS containing 0.1% Tween 20 (PBS-T). Blots were incubated in primary antibody at a 1:1000 dilution in blocking solution overnight at 4°C. Blots were washed three times for 10 min each in PBS-T and incubated in secondary antibody conjugated to horseradish peroxidase for 1 h at room temperature (1:3000 dilution; Sigma-Aldrich). Blots were washed again three times for 10 min each in PBS-T before visualization using SuperSignal chemiluminescent substrate (Pierce, Rockford, IL) and the VersaDoc Imaging System (Bio-Rad, Hercules, CA). Protein expression quantification was accomplished using densitometry software on the VersaDoc (Quality One; Bio-Rad).

LysoTracker staining/filipin costaining

Cells were grown to 75-90% confluency on Fisher brand glass coverslips. Cells incubated in 1 μM LysoTracker Red DND-99 (Molecular Probes, Eugene, OR) in normal growth medium for

3 h at 37°C at 95% O_2–5% CO_2. Then cells were rinsed three times with PBS and fixed with 2% paraformaldehyde for 30 min at room temperature. Again cells were rinsed three times with PBS and either mounted onto slides using SlowFade Light antifade (Molecular Probes) or stained with filipin as previously described. Cells were visualized in the 595–605 nm range for the LysoTracker or the UV range for the filipin using a wide-field microscope on a Zeiss Axiovert 200 and Metamorph software. A 40× objective was used for all images.

βarr2 shRNA transfection

The βarr2-shRNA-expressing vectors and respective negative control vector were obtained from Qiagen (Germantown, MD). Cells were seeded at a density of 200,000 cells per well in 6-well tissue culture dishes 24 h before transfection. Manufacturer protocol for transfection was followed. Briefly, for each transfection, 15 μl of Xtreme Gene 9 (Roche, Indianapolis, IN) was incubated for 10 min at room temperature in 100 μl of OptiMEM (Gibco, Carlsbad, CA). Concurrently for each transfection, 0.4 μg of DNA was incubated for 10 min at room temperature in 100 μl of OptiMEM (Gibco). Then Xtreme Gene/OptiMEM mix was added to DNA/OptiMEM mix, mixed gently, and incubated for an additional 20 min at room temperature. Finally, 100 μl of diluted transfection mix was added to each well containing 400 μl of normal growth medium, and cells were incubated at 37°C in 95% O_2–5% CO_2 for 48 h. Transfection media were removed, and 2 ml of fresh media containing 80 μg/ml hygromycin was added. Cells were maintained in the selection media until ready for screening. Cells were filipin stained and mounted as described previously. Cells were visualized in the UV range for the filipin on a Zeiss Axiovert 200 and Metamorph software. A 40× objective was used for all images.

NPC1 imaging studies

NPC1-mCherry constructs were obtained from Dr. Kevin Vaughan (University of Notre Dame, Notre Dame, IN).

Transfection. Cells were plated on vitrogen-coated coverslips at a density of 5×10^4 cells per coverslip in a 12-well dish. For each transfection, 0.6 Fugene (Roche, Indianapolis, IN) was added to 100 μl Optimem and incubated at room temperature (RT) for 5 min, after which 0.3 μg DNA was added and incubated at RT for 15 min. Plating media was removed and replaced with 400 μl fresh SF media and 100 μl of the transfection mix. Cells were allowed to incubate overnight at 37°C, 5% CO_2.

Live imaging. Vacuum grease was placed in a thin layer on a microscope slide roughly outlining the shape of the coverslips, and a small amount of media was added to the slide in this circle of vacuum grease. Coverslips were inverted onto the slide and visualized using a Zeiss Axiovert 200 (Jena, Germany) with a 40× oil objective and 500 ms exposure. Stacked images were taken using the Metamorph software (Molecular Devices, Sunnydale, CA). Live images were taken in stream acquisition mode at a rate of 1.4 frames/s. The three most mobile NPC1-tagged organelles in GFP-expressing cells were tracked for 25 frames.

Measuring cholesterol synthesis in vivo

Cholesterol synthesis measurements were performed as described (11). Briefly, mice and the matched controls were given an intraperitoneal injection (~24 μl per g body weight) of deuterated saline (9 g NaCl in 1,000 ml of 99% ^2H_2O; Sigma-Aldrich, St. Louis, MO). After 8 h, mice were euthanized using carbon dioxide. Blood was taken from the heart, and plasma was collected. Whole lungs and approximately 1.0 g of liver and small intestine were collected. Tissue samples were hydrolyzed in 1N KOH/70% ethanol (v/v) for 2 h at 70°C, vortexing occasionally. Samples were then evaporated to dryness, redissolved in 2 ml of water, and acidified using 12N HCl. Cholesterol was extracted twice by addition of ethyl ether (3 ml). The pooled ether extracts were evaporated to dryness under nitrogen and then converted to the trimethylsilyl cholesterol derivatives by reacting with 60 μl of bis(trimethylsilyl) trifluoroacetamide + 1% trimethylchlorosilane (TMS; Regis, Morton Grove, IL) at 60°C for 20 min. The ^2H-labeling of cholesterol was determined using an Agilent 5973N-MSD equipped with an Agilent 6890 GC system. The cholesterol was run on a DB17-MS capillary column (30 m × 0.25 mm × 0.25 μm). The oven temperature was initially held for 1 min at 150°C, then increased by 20°C per min to 310°C and maintained for 8 min. The split ratio was 20:1 with helium flow 1 ml per min. The inlet temperature was set at 270°C, and the MS transfer line was set at 310°C. Under these conditions, cholesterol elutes at ~11.1 min. Electron impact ionization was used in all analyses with selected ion monitoring of *m/z* 368–372 (M0–M4, =/cholesterol), dwell time of 10 ms per ion. Plasma was diluted 2-fold with distilled water and reacted with 2 μl of 10 N NaOH and 4 μl of a 5% (v/v) solution of acetone in acetonitrile for 24 h. Acetone was extracted by addition of 600 μl of chloroform, followed by addition of 0.5 g Na_2SO_4. Samples were vigorously mixed, and a small aliquot of the chloroform was transferred to a GC-MS vial. Acetone was analyzed using the Agilent equipment described above. The oven temperature program was 60°C initially, increased by 20°C per min to 100°C, increased by 50°C per min to 220°C, and maintain for 1 min. The split ratio was 40:1 with a helium flow of 1 ml per min. The inlet temperature was set at 230°C, and the MS transfer line was set at 245°C. Acetone eluted at ~1.5 min. The MS was operated in the electron impact mode (70 eV). Selective ion monitoring of *m/z* 58 and 59 was performed using a dwell time of 10 ms per ion.

RESULTS

Cholesterol processing in βarr2-overexpressing cells

The hypothesis of this study is that chronically elevated expression of βarr2 initiates pathways responsible for the cholesterol accumulation observed in CF cells. The first step in elucidating the role of βarr2 in cholesterol processing in CF is to determine whether exogenous βarr2 expression alone is enough to cause CF-like perinuclear cholesterol accumulation. 9/9/HTEo− cells stably expressing GFP-tagged βarr2 (βarr2-GFP cells) or stably expressing GFP alone (cont-GFP cells) were analyzed by filipin staining. The βarr2-GFP-expressing cells exhibit a clear perinuclear accumulation of free cholesterol that is similar to that seen in CF cells compared with respective controls (**Fig. 1**). These cells also show a colocalization of the expressed βarr2-GFP and unesterified cholesterol. Previous studies demonstrated that total βarr2 expression in βarr2-GFP cells was comparable to CF model cells (22).

Correction of cholesterol accumulation in βarr2-overexpressing cells with *Rp*-cAMPS

Previous data demonstrated that CF cholesterol accumulation could be reversed by treatment with the cAMP binding antagonist *Rp*-cAMPS (12). Because stable expression of βarr2 causes CF-like cholesterol accumulation in 9/9/HTEo− cells, it was tested whether cholesterol

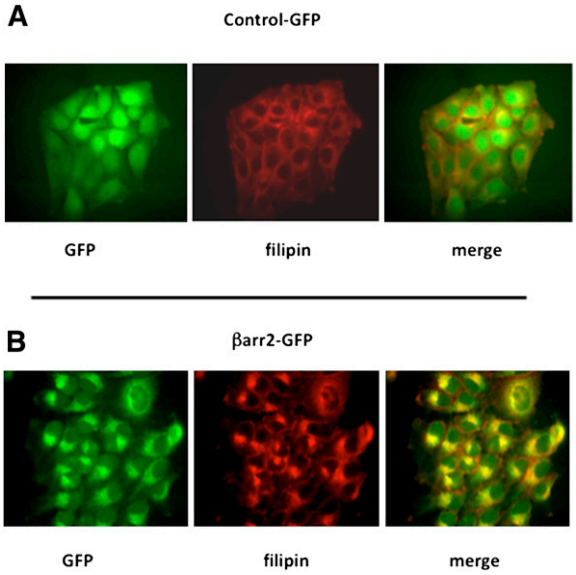

Fig. 1. Cholesterol accumulation in βarr2-expressing 9/9/HTEo− cells. (A) Representative images of GFP-expressing control cells stained for endogenous free cholesterol (filipin). (B) Representative images of GFP-tagged βarr2-expressing cells stained for endogenous free cholesterol (filipin). Images representative of at least 20 images for each cell type taken over three separate experiments.

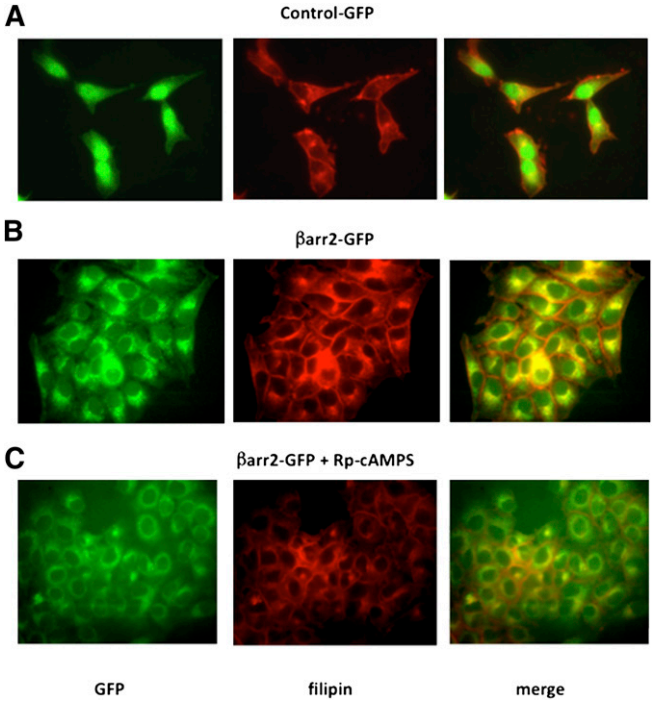

Fig. 2. Correction of cholesterol accumulation in βarr2-overexpressing cells with *Rp*-cAMPS (50 μM). (A) Representative image of untreated GFP-expressing (control-GFP) cells stained for endogenous free cholesterol (filipin). (B) Representative image of untreated βarr2-GFP cells stained for cholesterol (filipin). (C) Representative image of βarr2-GFP cells treated with *Rp*-cAMPS (50 μM) for 72 h and stained for cholesterol (filipin). Images are representative of at least 15 images for each condition taken over four separate experiments.

accumulation in βarr2-GFP cells exhibits the same *Rp*-cAMPS sensitivity observed in CF-model cells. βarr2-GFP cells were exposed to *Rp*-cAMPS (50 μM) for 24 h and 72 h, and then examined by filipin stain. Cholesterol accumulation in βarr2-GFP cells is reversed by *Rp*-cAMPS exposure, as is observed in CF cells (**Fig. 2**). Interestingly, βarr2-GFP localization is also redistributed in the presence of *Rp*-cAMPS, suggesting that a more general cellular trafficking defect may be involved in the accumulation phenotype.

Localization of βarr2-GFP and cholesterol

To determine whether βarr2-mediated cholesterol accumulation accurately models CF cholesterol accumulation, the localization of cholesterol accumulation between βarr2-GFP cells and CF IB3 cells was compared using the late endosomal/lysosomal marker LysoTracker (1 mM) and filipin staining. βarr2-GFP-expressing cells incubated in LysoTracker and filipin-stained show a colocalization of the βarr2, cholesterol, and LysoTracker (**Fig. 3**). IB3 cells also show a colocalization of cholesterol and LysoTracker, indicating that βarr2 expression is accurately recapitulating CF-related cholesterol processing characteristics (Fig. 3).

Effect of βarr2 knockdown on cholesterol accumulation

It is shown above that stable expression of βarr2 causes CF-like cholesterol accumulation. These data are consistent with previous findings in CF cells (12). It is possible that lipid accumulation in βarr2-GFP cells is the result of expressing increased amounts of protein in these cells as opposed to a specific effect of βarr2 expression, although GFP expression alone does not have this effect. To determine the full effect of βarr2 in the development of the CF cholesterol phenotype, shRNA was used to effectively knockdown βarr2 expression. CF IB3 cells stably transfected with βarr2 shRNA (clone 2) effectively reduced βarr2 expression as seen by Western blot analysis, whereas control shRNA and another βarr2 shRNA (clone 1) had no effect on βarr2 expression. These cell lines were examined by filipin staining to determine the effect of βarr2 expression on cholesterol accumulation (**Fig. 4**). IB3 control shRNA and IB3 clone 1 cells have CF-like perinuclear accumulation of cholesterol, whereas IB3 clone 2 cells (57% βarr2 expression compared with clone 1 as determined by densitometry) have a more dispersed pattern of cholesterol staining. These data indicate that cholesterol accumulation is in part dependent on βarr2 expression in CF-model cells, and depletion of βarr2 is enough to reverse the cholesterol phenotype.

Effect of in vivo depletion of βarr2 expression in *Cftr* $^{-/-}$ mice on cholesterol phenotypes

To verify the findings in the cellular studies above, a mouse model of βarr2 depletion was examined to further address the effect of βarr2 on cholesterol processing in CF. *Cftr/βarr2* double knockout (DKO) mice were developed as recently published (22) and utilized to directly examine the effect of βarr2 on aspects of cholesterol processing and signaling. We previously demonstrated that CF mice exhibit increased de novo cholesterol synthesis in the liver compared with sibling WT mice (11). We also

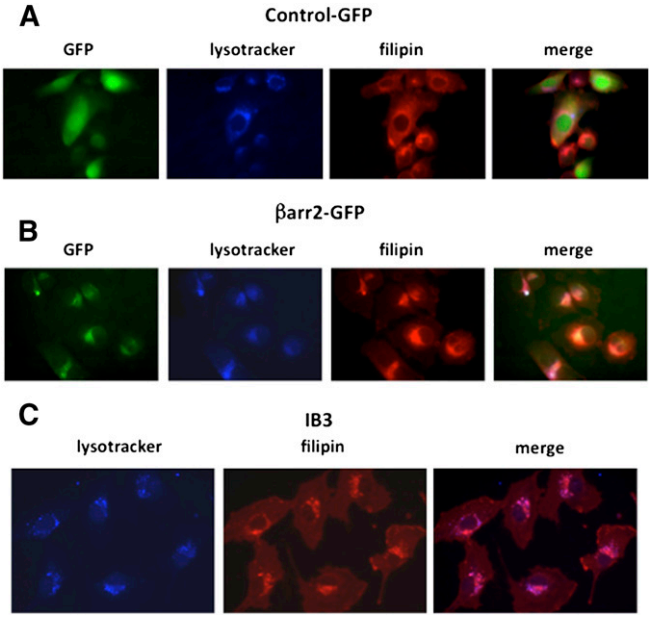

Fig. 3. Localization of cholesterol and βarr2 in the lysosomes in CF and βarr2-overexpressing cells. (A) Representative image of lysosomes (LysoTracker) and endogenous free cholesterol (filipin) in GFP-expressing control cells. (B) Representative image of lysosomes (LysoTracker) and endogenous free cholesterol (filipin) in βarr2-GFP cells. (C) Representative image of lysosomes (LysoTracker) and endogenous free cholesterol (filipin) in IB3 cells. Images are representative of at least 15 images for each condition taken over three separate experiments.

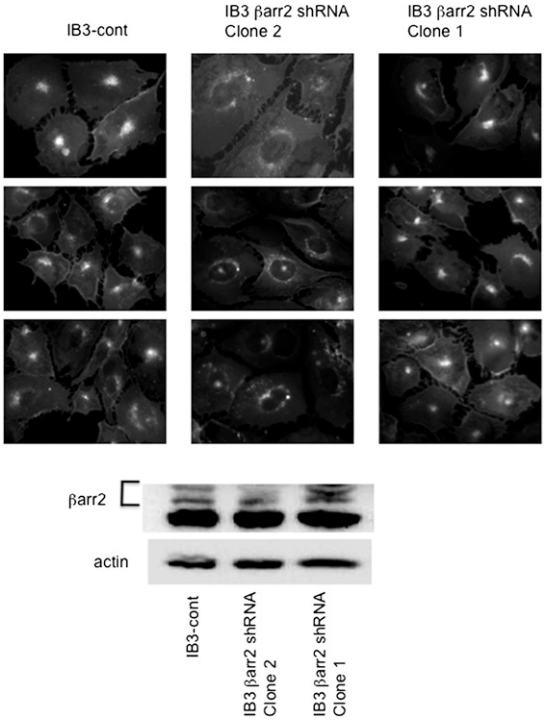

Fig. 4. Correction of cholesterol accumulation in IB3 cells using βarr2 shRNA. (A) Three representative images from three clonal cell lines [IB3-control shRNA, IB3-βarr2 shRNA (clone 2), and IB3-βarr2 shRNA (clone 1)]. Only clone 2 (βarr2 shRNA) depleted βarr2 expression. Images show endogenous free cholesterol distribution using filipin staining. Images are representative of at least 15 images for each condition taken over three separate experiments. (B) Representative Western blot image showing βarr2 expression. Image is representative of three separate experiments.

demonstrated that downstream signaling events, such as reduced NOS2 expression and increased RhoA expression, were directly related to cholesterol synthesis increases in mouse models of CF (23). These outcomes were examined in WT, *Cftr* $^{-/-}$, and *Cftr/βarr2* DKO mice as a measure of the influence of βarr2 on cholesterol-related events in an in vivo model of CF.

De novo cholesterol synthesis was measured in WT, *Cftr* $^{-/-}$, *Cftr/βarr2* DKO, and *βarr2* $^{-/-}$ mice using a D_2O labeling method as described. Percentage de novo cholesterol synthesis in *Cftr* $^{-/-}$ mice (20.9 ± 1.7, n = 7) was significantly greater than that observed in WT mice (12.9 ± 1.3, n = 8), consistent with previously published data (11). *Cftr/βarr2* DKO mice, however, exhibit de novo cholesterol synthesis levels (10.4 ± 1.1, n = 3) that were significantly lower than WT levels. Synthesis levels in βarr2 $^{-/-}$ mice (8.9 ± 0.4, n = 4) were also significantly lower than WT mice values, but they were not different from *Cftr/βarr2* DKO values (**Fig. 5**). Total cholesterol content in the liver was not significantly changed between groups. Significance between groups was determined by ANOVA analysis with the Newman-Keuls multiple comparison posthoc test ($P < 0.05$). These data demonstrate directly that depletion of βarr2 expression in a CF model reverts a quantifiable measure of cholesterol processing toward WT levels in vivo.

If de novo cholesterol synthesis rates are reverted toward WT levels in *Cftr/βarr2* DKO mice compared with *Cftr* $^{-/-}$ mice, then it is predicted that downstream events related to elevated cholesterol synthesis would also be reversed. To test this prediction, protein expression levels of NOS2 and RhoA were examined in the mouse models described above. Consistent with previous data, RhoA expression was significantly increased and NOS2 expression was significantly decreased in *Cftr* $^{-/-}$ MNE compared with WT samples (**Fig. 6A**). Expression patterns in *Cftr/βarr2* DKO samples, however, more closely resembled that of WT mice. Expression of RhoA and NOS2 in *βarr2* $^{-/-}$ mice resembled WT mice. The effect of βarr2 depletion in non-CF mice (*βarr2* $^{-/-}$) on NOS2 expression compared with WT mice was also examined. Relative NOS2/actin expression in *βarr2* $^{-/-}$ mice was 1.3 ± 0.4-fold increased compared with WT mice (1.0; n = 3; not significant). These data provide further evidence that βarr2 expression is a key to mediating cholesterol-related phenotypes in CF.

Fig. 2 demonstrates that βarr2-mediated cholesterol accumulation is sensitive to *Rp*-cAMPS treatment, as is observed in CF-cell models (12), suggesting that *Rp*-cAMPS and βarr2 are acting within the same pathway. If βarr2 depletion in CF models is acting like *Rp*-cAMPS treatment regarding cholesterol processing, then the effect of in vivo treatment of *Cftr* $^{-/-}$ mice with *Rp*-cAMPS should mimic the results observed in *Cftr/βarr2* DKO mice. To test this hypothesis, the marker of NOS2 expression was examined in MNE from *Cftr* $^{-/-}$ mice treated with *Rp*-cAMPS (5 mg/kg/day for 12 days). As was observed in *Cftr/βarr2* DKO

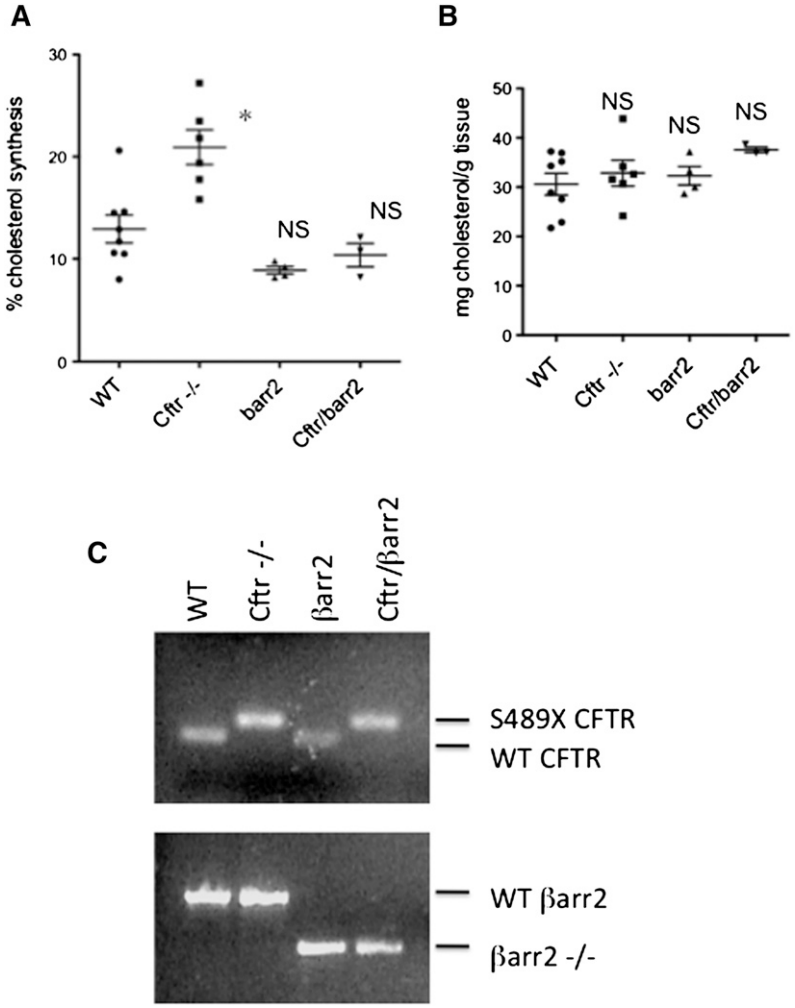

Fig. 5. De novo cholesterol synthesis in WT, *Cftr* $^{-/-}$, *barr2* $^{-/-}$, and *Cftr/barr2* DKO mice. (A) Scatterplot of liver de novo cholesterol synthesis in each model system. (B) Scatterplot of total liver cholesterol content in each model system. Significance determined by ANOVA. Comparisons between groups were performed with the Newman-Keuls posthoc test. *$P < 0.05$; NS = not significant compared with WT mice. (C) Representative gels demonstrating genotyping performed on each mouse.

mice, NOS2 expression in *Rp*-cAMPS-treated *Cftr* $^{-/-}$ mice returned to WT levels (Fig. 6B).

Examination of organelle trafficking in a cultured CF-cell model

Cholesterol accumulation in both CF cells and βarr2-GFP 9/9/HTEo− cells is reversible by treatment with *Rp*-cAMPS, suggesting that similar mechanisms leading to accumulation are involved in each cell type. Ko et al. demonstrated that cholesterol accumulation in U18666a-treated cells corresponded to reduced vectorial movement of NPC1-containing organelles (24). U18666a is an inhibitor of cholesterol processing and of cholesterol synthesis often used to induce cholesterol accumulation. It is hypothesized that cholesterol accumulation in CF cells is not due to a specific flaw in cholesterol transport but to diminished vectorial or outward movement of endosomes in CF cells. To test the hypothesis that reduced organelle movement leads to cholesterol accumulation in CF-model cells and is *Rp*-cAMPS sensitive, studies were performed by transfecting WT and CF-model cells with a construct expressing an mCherry-labeled NPC1 protein obtained from Dr. Kevin Vaughan (University of Notre Dame), and vectorial movement assessed using live cell imaging. WT cells exhibit an even dispersal of organelles with free, rapid movement (**Fig. 7**). CF-model cells, however, exhibit a clustering of NPC1-labeled organelles near the nucleus, consistent with cholesterol accumulation data and restricted movement. CF-model cells treated with *Rp*-cAMPS, a compound we have shown to alleviate cholesterol accumulation in CF (3), exhibit improved organelle dispersion and an increase in maximal movement. These data suggest that cholesterol accumulation in CF is due to lack of organelle trafficking. Quantification of NPC1-mCherry-labeled organelles is shown in Fig. 7B. Values for each condition are WT pCEP-9/9/HTEo− (37.8 ± 2.2, n = 80); CF-model pCEPR-9/9/HTEo− (20.6 ± 2.4, n = 51); CF-model cells plus 50 μM *Rp*-cAMPS from 48 h (30.2 ± 5.3, n = 29); and WT cells plus 1 μM nocodazole (13.8 ± 2.2, n = 21). These data demonstrate directly that organelle trafficking is interrupted in CF-model cells and that *Rp*-cAMPS is capable of reversing this phenotype at least toward WT levels. Nocodazole treatment of WT cells is shown as a control for disruption of microtubule-mediated vectorial transport.

As βarr2 expression appears to be a key regulator of cholesterol processing, the hypothesis that organelle transport efficiency also is regulated by βarr2 was examined. Using the same NPC1-mCherry approach, we analyzed organelle movement in βarr2-GFP 9/9/HTEo− cells compared with GFP-expressing 9/9/HTEo− controls. As shown in **Fig. 8**,

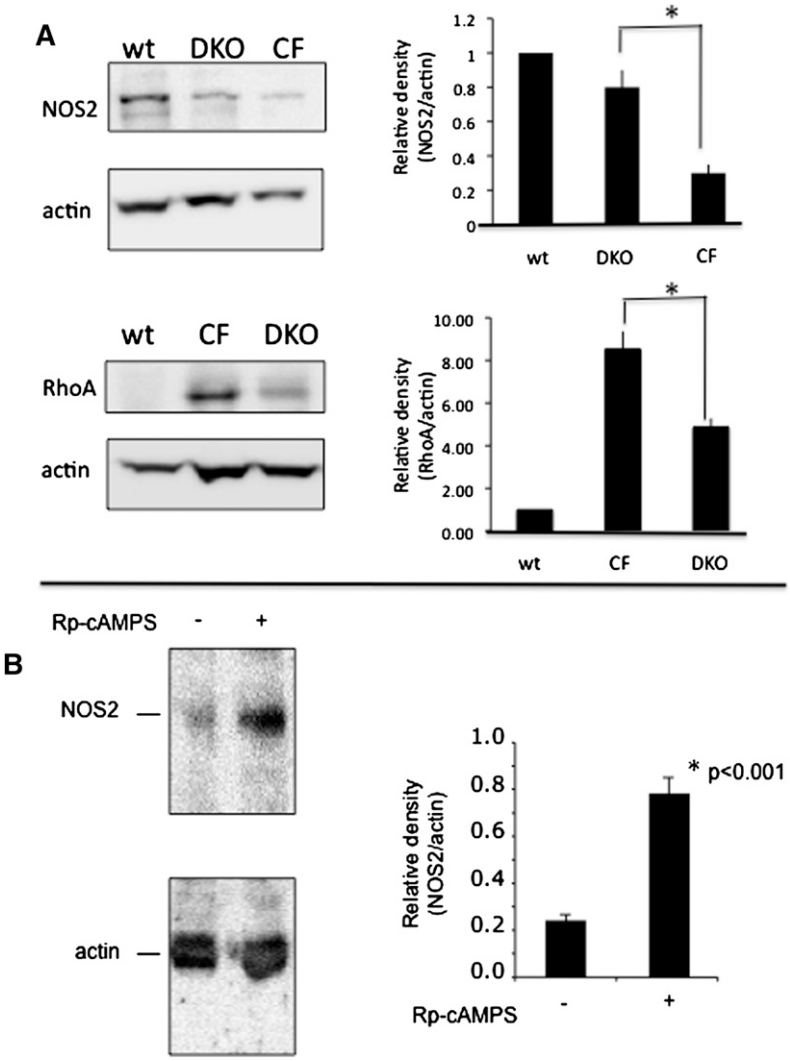

Fig. 6. Effect of βarr2 deletion on signaling protein expression in CF mouse nasal epithelium. (A) The expression of NOS2 and RhoA were examined in sibling WT mice (n = 6), *Cftr* $^{-/-}$ (CF) mice (n = 4), and *Cftr* $^{-/-}$; *barr2* $^{-/-}$ DKO mice (n = 5). Significance determined by ANOVA. Comparisons between groups was performed with the Newman-Keuls post-hoc test; $*P < 0.05$. (B) The effect of *Rp*-cAMPS on NOS2 expression in *Cftr* $^{-/-}$ mouse nasal epithelium. *Cftr* $^{-/-}$ mice were treated with either saline or *Rp*-cAMPS for 12 days and assayed for NOS2 expression normalized to actin content. Significance determined by *t*-test; n = 10 for each group.

βarr2-GFP-expressing cells exhibit identical reduction in vesicular movement as observed in CF-model cells. Cont-GFP 9/9/HTEo− cells (28.3 ± 2.2, n = 48) compared with βarr2-GFP 9/9/HTEo− cells (19.9 ± 1.4, n = 54). These data point to a specific mechanism by which βarr2 can influence the phenotype of cholesterol accumulation in CF cells.

DISCUSSION

Several studies have revealed cholesterol-processing issues in CF cells (10–12, 25–27). Studies by Gentsch et al. suggest that misfolding of ΔF508 CFTR leads to lipid accumulation (25). Our initial studies, however, demonstrate that *Cftr* $^{-/-}$ mice exhibit cholesterol-processing defects, suggesting that loss of CFTR function is a key to trafficking issues in CF cells (10–12). Previous findings demonstrated that protein expression levels of βarr2 are significantly elevated in cultured CF cells, nasal tissue from *Cftr* $^{-/-}$ mice, and from nasal scrapes obtained from CF subjects compared with expression in respective controls (12). It was also demonstrated that β2-AR colocalizes with cholesterol in cultured CF-model cells, one of multiple GPCRs internalized by the GRK/arrestin pathway (12). These data led to the hypothesis of this study that βarr2 expression is a key regulator of organelle trafficking in CF cells, leading to cholesterol accumulation.

Note that cholesterol accumulation is likely only a marker of a more pronounced defect in organelle trafficking in CF, as other cellular components have been shown to accumulate in the late endosomes/lysosomes. As mentioned above, we have demonstrated that β2-AR colocalizes with cholesterol in the perinuclear region (12). Recently Bruscia et al. have shown in CF macrophages that toll-like receptor-4 (TLR4) accumulates in endosomes, leading to increased cytokine production (28). Further evidence of altered organelle movement can be seen in a study by Luciani et al. showing that defective CFTR leads to decreased aggresome clearance and defective autophagy (29). Aggresome formation has been reported previously in CF studies in response to ΔF508 misfolding and aggregation (30). The study by Luciani et al. demonstrates that deficiency of CFTR can have similar trafficking and organelle regulatory effects that have been previously only attributed to mutant CFTR misfolding, indicating that loss of CFTR function and increased expression of ΔF508 CFTR can have similar impacts on cellular trafficking patterns (29). These findings explain how overexpressing ΔF508 in a

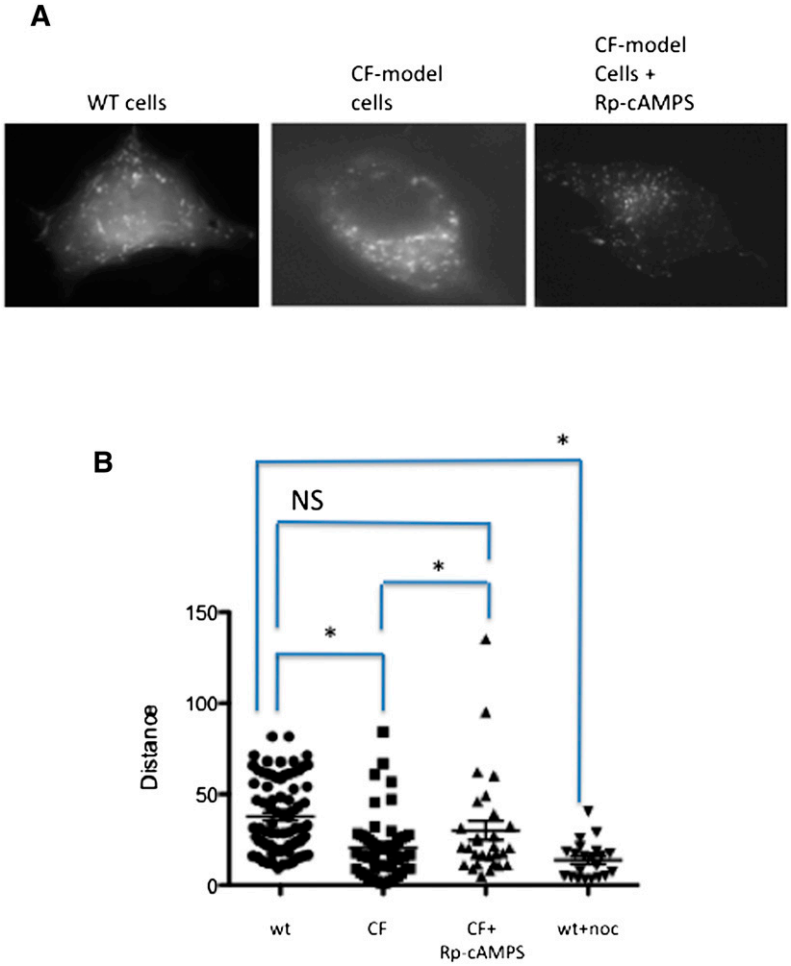

Fig. 7. Organelle trafficking in WT and CF-model cells using NPC1-mcherry as a marker. (A) Still frames from video of NPC1-labeled organelle movement. (B) Quantification of NPC1-mCherry-labeled organelle mobility. The three most mobile organelles from cells over five separate experiments were analyzed for relative distance moved. Nocodazole (noc; 50 nM) was used a positive control for disruption of MT-mediated transport. Significance determined by ANOVA. Comparisons between groups was performed with the Newman-Keuls posthoc test. $*P < 0.05$; NS = not significant.

study by Gentsch et al. and studies from our group using *Cftr* $^{-/-}$ mice and non-ΔF508 CFTR cell models can show cholesterol processing changes.

Mechanistically, data demonstrate that NPC1-containing vesicles are not trafficked efficiently in CF-model cells and that *Rp*-cAMPS treatment improves organelle mobility. Cholesterol accumulation in βarr2-GFP-expressing cells is also *Rp*-cAMPS sensitive, suggesting the possibility that elevated βarr2 expression may be affecting microtubule structure or transport. Shankar et al. have demonstrated that nonvisual arrestins associate directly with γ-tubulin in centrosomes and influence centrosome function as well as microtubule elongation (31). It is possible that increased expression of βarr2 in the centrosomal region enhances retrograde transport and leads to less efficient anterograde endosomal transport, visualized in these studies as perinuclear cholesterol accumulation. The role of βarr2 in regulating organelle transport and where *Rp*-cAMPS affects this process are areas in need of further investigation. It is also unclear whether the effect of arrestin expression on organelle movement or cholesterol processing is specific for βarr2. Both βarr1 and βarr2 interact with γ-tubulin and internalize GPCRs (31). Whether βarr1 has a similar effect needs to further explored.

These studies lead to the conclusion that βarr2 expression is key to the development of cholesterol-related phenotypes in CF cells. Cellular studies show that expression of βarr2-GFP in 9/9/HTEo− cells leads to CF-like cholesterol accumulation in late endosomal/lysosomal organelles. Expression of βarr2 shRNA in CF IB3 cells reduces cholesterol accumulation, and depletion of βarr2 expression in a CF mouse model reduces cholesterol synthesis rates to WT levels. We have previously demonstrated that newly synthesized cholesterol in CF cells is stored in the plasma membrane, resulting in an approximately 2-fold increase of cholesterol that is accessible to electrochemical detection (26). Whether βarr2 expression is a key factor in this observation is under investigation. Signaling protein profiles

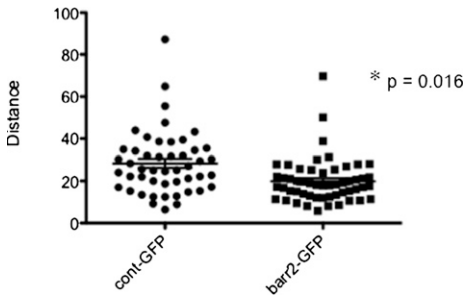

Fig. 8. Quantification of NPC1-mCherry-labeled organelle mobility control and βarr2-GFP expressing 9/HTEo cells. The three most mobile organelles from cells over duplicate experiments were analyzed for relative distance moved. Significance determined by *t*-test; $*P < 0.001$.

characteristic of CF (increased RhoA and decreased NOS2 protein expression) known to be related to the cholesterol pathway are also reversed toward WT levels in CF mouse nasal tissue in the absence of βarr2 expression. Accumulation of cholesterol mediated by βarr2 expression is reversible with *Rp*-cAMPS, as is observed in CF-cell models, with regulation of organelle trafficking proposed as a potential mechanism. Studies to identify the mechanisms leading to increased expression of βarr2 in CF cells and to determine how βarr2 mediates the effects on cholesterol transport are currently being performed. Understanding the role of βarr2-mediated involvement in cholesterol regulation in these diseases will lead to a better understanding of pathological processes in these diseases and illuminate new areas of intervention.

The authors thank Dr. Pam Davis, Case Western Reserve University, for providing cell lines necessary for completion of this study and Dr. Robert Lefkowitz, Howard Hughes Medical Institute, Duke University, for providing the GFP-tagged βarr2 construct and βarr2 null mice. The authors also thank Dr. Kevin Vaughan, University of Notre Dame, for providing the NPC1-mCherry construct. The authors thank Leigh Henderson and P. Bead for technical assistance.

REFERENCES

1. Drumm, M. L., H. A. Pope, W. H. Cliff, J. M. Rommens, S. A. Marvin, L. C. Tsui, F. S. Collins, R. A. Frizzell, and J. M. Wilson. 1990. Correction of the cystic fibrosis defect in vitro by retrovirus-mediated gene transfer. *Cell.* **62:** 1227–1233.
2. Drumm, M. L., D. J. Wilkinson, L. S. Smit, R. T. Worrell, T. V. Strong, R. A. Frizzell, D. C. Dawson, and F. S. Collins. 1991. Chloride conductance expressed by delta F508 and other mutant CFTRs in Xenopus oocytes. *Science.* **254:** 1797–1799.
3. Gregory, R. J., S. H. Cheng, D. P. Rich, J. Marshall, S. Paul, K. Hehir, L. Ostedgaard, K. W. Klinger, M. J. Welsh, and A. E. Smith. 1990. Expression and characterization of the cystic fibrosis transmembrane conductance regulator. *Nature.* **347:** 382–386.
4. Bear, C. E., C. H. Li, N. Kartner, R. J. Bridges, T. J. Jensen, M. Ramjeesingh, and J. R. Riordan. 1992. Purification and functional reconstitution of the cystic fibrosis transmembrane conductance regulator (CFTR). *Cell.* **68:** 809–818.
5. Tabary, O., J. M. Zahm, J. Hinnrasky, J. P. Couetil, P. Cornillet, M. Guenounou, D. Gaillard, E. Puchelle, and J. Jacquot. 1998. Selective up-regulation of chemokine IL-8 expression in cystic fibrosis bronchial gland cells in vivo and in vitro. *Am. J. Pathol.* **153:** 921–930.
6. Kelley, T. J., and H. L. Elmer. 2000. In vivo alterations of IFN regulatory factor-1 and PIAS1 protein levels in cystic fibrosis epithelium. *J. Clin. Invest.* **106:** 403–410.
7. Venkatakrishnan, A., A. A. Stecenko, G. King, T. R. Blackwell, K. L. Brigham, J. W. Christman, and T. S. Blackwell. 2000. Exaggerated activation of nuclear factor-kappaB and altered IkappaB-beta processing in cystic fibrosis bronchial epithelial cells. *Am. J. Respir. Cell Mol. Biol.* **23:** 396–403.
8. Chmiel, J. F., and M. W. Konstan. 2007. Inflammation and anti-inflammatory therapies for cystic fibrosis. *Clin. Chest Med.* **28:** 331–346.
9. Hunter, M. J., K. J. Treharne, A. K. Winter, D. M. Cassidy, S. Land, and A. Mehta. 2010. Expression of wild-type CFTR suppresses NF-kappaB-driven inflammatory signalling. *PLoS ONE.* **5:** e11598.
10. White, N. M., D. A. Corey, and T. J. Kelley. 2004. Mechanistic similarities between cultured cell models of cystic fibrosis and Niemann-Pick type C. *Am. J. Respir. Cell Mol. Biol.* **31:** 538–543.
11. White, N. M., D. Jiang, J. D. Burgess, I. R. Bederman, S. F. Previs, and T. J. Kelley. 2007. Altered cholesterol homeostsis in cultured and *in vivo* models of cystic fibrosis. *Am. J. Physiol. Lung Cell. Mol. Physiol.* **292:** L476–L486.
12. Manson, M. E., D. A. Corey, N. M. White, and T. J. Kelley. 2008. cAMP-mediated regulation of cholesterol accumulation in cystic fibrosis and Niemann-Pick type C cells. *Am. J. Physiol. Lung Cell. Mol. Physiol.* **295:** L809–L819.
13. Violin, J. D., X. R. Ren, and R. J. Lefkowitz. 2006. G-protein-coupled receptor kinase specificity for beta-arrestin recruitment to the beta2-adrenergic receptor revealed by fluorescence resonance energy transfer. *J. Biol. Chem.* **281:** 20577–20588.
14. Barnes, W. G., E. Reiter, J. D. Violin, X. R. Ren, G. Milligan, and R. J. Lefkowitz. 2005. beta-Arrestin 1 and Galphaq/11 coordinately activate RhoA and stress fiber formation following receptor stimulation. *J. Biol. Chem.* **280:** 8041–8050.
15. Povsic, T. J., T. A. Kohout, and R. J. Lefkowitz. 2003. Beta-arrestin1 mediates insulin-like growth factor 1 (IGF-1) activation of phosphatidylinositol 3-kinase (PI3K) and anti-apoptosis. *J. Biol. Chem.* **278:** 51334–51339.
16. Gesty-Palmer, D., M. Chen, E. Reiter, S. Ahn, C. D. Nelson, S. Wang, A. E. Eckhardt, C. L. Cowan, R. F. Spurney, L. M. Luttrell, et al. 2006. Distinct beta-arrestin- and G protein-dependent pathways for parathyroid hormone receptor-stimulated ERK1/2 activation. *J. Biol. Chem.* **281:** 10856–10864.
17. Parameswaran, N., C. S. Pao, K. S. Leonhard, D. S. Kang, M. Kratz, S. C. Ley, and J. L. Benovic. 2006. Arrestin-2 and G protein-coupled receptor kinase 5 interact with NFkappaB1 p105 and negatively regulate lipopolysaccharide-stimulated ERK1/2 activation in macrophages. *J. Biol. Chem.* **281:** 34159–34170.
18. Mak, J. C., T. T. Chuang, C. A. Harris, and P. J. Barnes. 2002. Increased expression of G protein-coupled receptor kinases in cystic fibrosis lung. *Eur. J. Pharmacol.* **436:** 165–172.
19. Sharma, R. K., and P. K. Jeffrey. 1990. Airway beta-adrenoceptor number in cystic fibrosis and asthma. *Clin. Sci. (Lond.).* **78:** 409–417.
20. Perez, A., K. A. Risma, E. A. Eckman, and P. B. Davis. 1996. Overexpression of R domain eliminates cAMP-stimulated Cl^- secretion in 9/HTEo- cells in culture. *Am. J. Physiol.* **271:** L85–L92.
21. Kruth, H. S., M. E. Comly, J. D. Butler, M. T. Vanier, J. K. Fink, D. A. Wenger, S. Patel, and P. G. Pentchev. 1986. Type C Niemann-Pick disease: abnormal metabolism of low density lipoprotein in homozygous and heterozygous fibroblasts. *J. Biol. Chem.* **261:** 16769–16774.
22. Manson, M. E., D. A. Corey, S. M. Rymut, and T. J. Kelley. 2011. β-arrestin-2 regulation of the cAMP response element binding protein. *Biochemistry.* **50:** 6022–6029.
23. Kreiselmeier, N. E., N. C. Kraynack, D. A. Corey, and T. J. Kelley. 2003. Statin-mediated correction of Stat1 signaling and inducible nitric oxide synthase expression in cystic fibrosis epithelial cells. *Am. J. Physiol. Lung Cell Mol. Physiol.* **285:** L1286–L1295.
24. Ko, D. C., M. D. Gordon, J. Y. Jin, and M. P. Scott. 2001. Dynamic movements of organelles containing Niemann-Pick C1 protein: NPC1 involvement in late endocytic events. *Mol. Biol. Cell.* **12:** 601–614.
25. Gentzsch, M., A. Choudhury, X. B. Chang, R. E. Pagano, and J. R. Riordan. 2007. Misassembled mutant DeltaF508 CFTR in the distal secretory pathway alters cellular lipid trafficking. *J. Cell Sci.* **120:** 447–455.
26. Fang, D., R. H. West, M. E. Manson, J. Ruddy, D. Jiang, S. F. Previs, N. D. Sonawane, J. D. Burgess, and T. J. Kelley. 2010. Increased plasma membrane cholesterol in cystic fibrosis cells correlates with CFTR genotype and depends on de novo cholesterol synthesis. *Respir. Res.* **11:** 61.
27. Lim, C. H., M. J. Bijvelds, A. Nigg, K. Schoonderwoerd, A. B. Houtsmuller, H. R. de Jonge, and B. C. Tilly. 2007. Cholesterol depletion and genistein as tools to promote F508delCFTR retention at the plasma membrane. *Cell. Physiol. Biochem.* **20:** 473–482.
28. Bruscia, E. M., P. X. Zhang, A. Satoh, C. Caputo, R. Medzhitov, A. Shenoy, M. E. Egan, and D. S. Krause. 2011. Abnormal trafficking and degradation of TLR4 underlie the elevated inflammatory response in cystic fibrosis. *J. Immunol.* **186:** 6990–6998.
29. Luciani, A., V. R. Villella, S. Esposito, N. Brunetti-Pierri, D. Medina, C. Settembre, M. Gavina, L. Pulze, I. Giardino, M. Pettoello-Mantovani, et al. 2010. Defective CFTR induces aggresome formation and lung inflammation in cystic fibrosis through ROS-mediated autophagy inhibition. *Nat. Cell Biol.* **12:** 863–875.
30. Johnston, J. A., C. L. Ward, and R. R. Kopito. 1998. Aggresomes: a cellular response to misfolded proteins. *J. Cell Biol.* **143:** 1883–1898.
31. Shankar, H., A. Michal, R. C. Kern, D. S. Kang, V. V. Gurevich, and J. L. Benovic. 2010. Non-visual arrestins are constitutively associated with the centrosome and regulate centrosome function. *J. Biol. Chem.* **285:** 8316–8329.